
Proceedings Paper:
Dai, M., Ma, X., Liu, W. orcid.org/0000-0003-2968-2888 et al. (1 more author) (2020) Polarization parameters estimation with scalar sensor arrays. In: Proceedings of the 45th IEEE International Conference on Acoustics, Speech, and Signal Processing. ICASSP 2020 : 45th IEEE International Conference on Acoustics, Speech, and Signal Processing, 04-08 May 2020, Barcelona, Spain. IEEE , pp. 4667-4671. ISBN 9781509066322

https://doi.org/10.1109/ICASSP40776.2020.9053818

POLARIZATION PARAMETERS ESTIMATION WITH SCALAR SENSOR ARRAYS

Minghui Dai[†], *Xiaofeng Ma*[† §], *Wei Liu*[§], *Weixing Sheng*[†]

[†] School of Electronic Engineering and Optoelectronic Technology, Nanjing University of Science and Technology, Nanjing 210094, China

[§] Department of Electronic and Electrical Engineering, University of Sheffield Sheffield, S1 3JD, United Kingdom

ABSTRACT

The scalar sensor array (SSA) is generally assumed insensitive to the polarization of impinging signals, and only diversely polarized arrays, such as the vector (crossed-dipole or tripole) sensor array (VSA), can be used for polarization estimation. However, as shown in this paper, with the mutual coupling effect, the SSA can become partially sensitive to polarization of the impinging signals and therefore can be used for polarization parameter estimation. The polarization sensitivity model of an SSA is first established and then as an example, a dimension-reduction method based on multiple signal classification (MUSIC) is employed to jointly estimate the direction-of-arrival and polarization parameters. Computer simulations based on a planar array of circularly polarized microstrip antennas are provided to demonstrate the performance of the proposed method.

Index Terms— scalar sensor array, polarization sensitivity, mutual coupling.

1. INTRODUCTION

Polarization parameter estimation plays an important role in a wide range of antenna array applications and two representative examples are its application for target identification in radar systems and capacity improvement in wireless communication systems [1]-[4]. The traditional scalar sensor arrays (SSAs), which employ identical single-output antennas, are generally considered as polarization insensitive arrays in almost all the literature [5]-[7]. As a result, they can only be used for direction-of-arrival (DOA) estimation of impinging signals rather than polarization estimation. In order to estimate the polarization information, polarization sensitive vector sensor arrays (VSAs), such as crossed-dipole arrays and tripole arrays, have to be employed [8]-[12].

Recent research indicates that the SSA has certain degrees of polarization sensitivity under the mutual coupling effect [13], which alters the beam pattern of each individual antenna in different ways [14]. Therefore, it becomes possible to estimate the polarization parameters based on traditional SSA structures.

In this paper, the polarization estimation model based on an SSA with mutual coupling is established first and the problem is solved by a MUSIC based algorithm as a representative example [16], [17]. To reduce the computational complexity of simultaneous four-dimensional (4-D) search, similar to [17], a dimension-reduction method is employed to decompose it into two separate two-dimensional (2-D) searches. Firstly, the accurate beam response of horizontal and vertical components of each antenna in the SSA is obtained by an electromagnetic (EM) full-wave simulation software, such as the Ansys HFSS [18]. With the obtained polarization sensitivity information, an EM wave receiving model for such an SSA is established. Finally, the dimension-reduction based MUSIC algorithm is derived to estimate both the polarization parameters and DOA parameters. In the simulations part, a planar array of 16 right circularly polarized microstrip antennas is employed to show the feasibility of the proposed method for estimating both the DOA and polarization parameters with SSAs. The direct relationship between estimation accuracy and polarization sensitivity is also demonstrated through computer simulations.

The rest of the paper is organized as follows. The SSA model with polarization sensitivity analysis is introduced in Section 2, and the dimension-reduction MUSIC method is derived in Section 3. Simulation results are provided in Section 4, and conclusions are drawn in Section 5.

2. SSA MODEL WITH POLARIZATION SENSITIVITY

2.1. Polarization of EM Signals

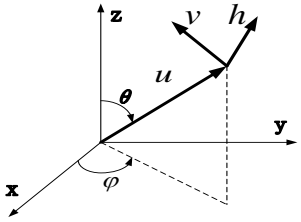

Fig. 1. The orthonormal vector triad of an EM wave.

A planar EM wave received by an antenna array has an electric field $\boldsymbol{E}$ and a magnetic field $\boldsymbol{H}$ that are orthogonal to the direction of propagation defined by the unit direction vector $\boldsymbol{u}(\theta,\varphi)$, where θ is the elevation angle and φ is the azimuth angle. The relationship between $\boldsymbol{E}$ and $\boldsymbol{H}$ can be expressed as

$$\boldsymbol{H} = -\frac{1}{\eta}\boldsymbol{u}\times\boldsymbol{E} \tag{1}$$

where η is the intrinsic impedance of the medium. The electric and magnetic fields are orthogonal to each other, allowing them to be represented reciprocally [19], and thus the polarization of an EM wave can be defined as the orientation of the electric field vector, as shown in Fig. 1.

The vectors $\boldsymbol{h}$ and $\boldsymbol{v}$ are defined as the horizontal and vertical polarized components of the electric fields, respectively, which form a right-handed orthonormal basis [20].

$$\begin{aligned}\boldsymbol{u} &= [\sin\theta\cos\varphi, \sin\theta\sin\varphi, \cos\theta]^T\\ \boldsymbol{h} &= [-\sin\varphi, \cos\varphi, 0]^T\\ \boldsymbol{v} &= [\cos\theta\cos\varphi, \cos\theta\sin\varphi, -\sin\theta]^T\end{aligned} \tag{2}$$

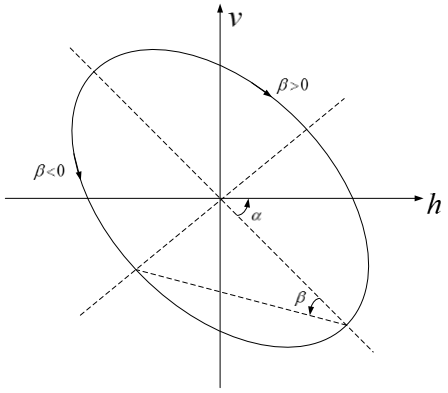

Fig. 2. Electric polarization ellipse.

The electric field vector of the incoming wave signal moves on an electric polarization ellipse, as shown in Fig. 2. The ellipse is described by the orientation angle $\alpha \in (-\pi/2, \pi/2]$ and the ellipticity angle $\beta \in [-\pi/4, \pi/4]$. Then, the normalized electric vector $\boldsymbol{E}(t)$ can be expressed as

$$\begin{aligned}\boldsymbol{E}(t) &= \begin{bmatrix}\boldsymbol{E}_H(t) & \boldsymbol{E}_V(t)\end{bmatrix}^T = \boldsymbol{p}(\alpha,\beta)s(t)\\ &= \begin{bmatrix}\cos\alpha & -\sin\alpha\\ \sin\alpha & \cos\alpha\end{bmatrix}\begin{bmatrix}\cos\beta\\ j\sin\beta\end{bmatrix}s(t)\end{aligned} \tag{3}$$

where $\boldsymbol{E}_H(t)$ and $\boldsymbol{E}_V(t)$ are the horizontal and vertical electric fields, respectively, $s(t)$ denotes the transmitted scalar signal, and $\boldsymbol{p}(\alpha,\beta)$ is the polarization vector representing the signal polarization characteristics. As a result, an arbitrary polarization state can be uniquely represented by α and β. For example, the transmission is of linear polarization with $\beta = 0$ and circular polarization with $|\beta| = \pi/4$.

2.2. The SSA Model

Assume that K far-field stationary and narrowband polarized signals from direction angles (θ_k,φ_k) impinge on an array of M sensors placed at arbitrary but known locations $\boldsymbol{r}_m=(x_m, y_m, z_m)$, $m = 1, \ldots, M$, with $K < M$. The array output vector $\boldsymbol{x}(t)$ of $M\times 1$ is expressed as

$$\boldsymbol{x}(t) = \sum_{k=1}^{K}\boldsymbol{A}(\theta_k,\varphi_k)\boldsymbol{p}(\alpha_k,\beta_k)s_k(t) + \boldsymbol{n}(t) \tag{4}$$

where $\boldsymbol{n}(t)$ is the zero-mean additive noise vector, $\boldsymbol{p}(\alpha_k,\beta_k)$ is the polarization vector of the kth signal $s_k(t)$ and $\boldsymbol{A}(\theta_k,\varphi_k)$ is the $M\times 2$ array manifold matrix, given by

$$\begin{aligned}\boldsymbol{A}(\theta_k,\varphi_k) &= \begin{bmatrix}\boldsymbol{a}_H(\theta_k,\varphi_k) & \boldsymbol{a}_V(\theta_k,\varphi_k)\end{bmatrix}\\ &= \begin{bmatrix}\boldsymbol{f}_H(\theta_k,\varphi_k)\,\square\,\boldsymbol{a}_S(\theta_k,\varphi_k) & \boldsymbol{f}_V(\theta_k,\varphi_k)\,\square\,\boldsymbol{a}_S(\theta_k,\varphi_k)\end{bmatrix}\end{aligned} \tag{5}$$

where $\boldsymbol{f}_H(\theta_k,\varphi_k) = [g_{H\_1}(\theta_k,\varphi_k),\ldots, g_{H\_M}(\theta_k,\varphi_k)]^T$ and $\boldsymbol{f}_V(\theta_k,\varphi_k) = [g_{V\_1}(\theta_k,\varphi_k),\ldots, g_{V\_M}(\theta_k,\varphi_k)]^T$ are the horizontal and vertical components of the embedded antenna gain of M sensors for (θ_k,φ_k), respectively. $g_{H\_m}(\theta,\varphi)$ and $g_{v\_m}(\theta,\varphi)$ are two components of the mth embedded element pattern. $\square$ is the Hadmard product. $\boldsymbol{a}_s(\theta_k,\varphi_k)$ is the spatial steering vector of the array

$$\boldsymbol{a}_s(\theta_k,\varphi_k) = [\mathrm{e}^{jk_0\boldsymbol{r}_1\cdot\boldsymbol{u}(\theta_k,\varphi_k)},\ldots,\mathrm{e}^{jk_0\boldsymbol{r}_M\cdot\boldsymbol{u}(\theta_k,\varphi_k)}]^T \tag{6}$$

where $k_0 = 2\pi/\lambda$ is the wave number, and λ is the wavelength.

Traditionally, as mentioned above, the antenna polarization characteristics in an SSA are generally considered to be consistent among all elements, which means basically there is no interaction or mutual coupling between antennas in the array [6]. In other words, the two corresponding components of all embedded element patterns are the same. The polarizations of each antenna in all directions are also the same, given by

$$g_{H\_1}(\theta,\varphi) = g_{H\_2}(\theta,\varphi) = \cdots = g_{H\_M}(\theta,\varphi) \tag{7a}$$

$$g_{V\_1}(\theta,\varphi) = g_{V\_2}(\theta,\varphi) = \cdots = g_{V\_M}(\theta,\varphi) \tag{7b}$$

$$\frac{g_{H\_m}(\theta,\varphi)}{g_{V\_m}(\theta,\varphi)} = \gamma, \qquad m = 1,\ldots,M \tag{7c}$$

where γ is a complex constant.

Then, $\boldsymbol{A}(\theta_k,\varphi_k)$=$g_{H\_m}(\theta_k,\varphi_k)\cdot\boldsymbol{a}_S(\theta_k,\varphi_k)\cdot[1 \quad \gamma]$ is a rank-1 matrix. The array manifold in (5) does not carry any polarization information.

However, the result will change when the mutual coupling effect is taken into consideration. The electric field of each antenna changes due to the interaction with other adjacent antennas. Thus, the beam pattern of the antennas

differs from each other, leading to a polarization dependent antenna response, which is reflected in both the horizontal and vertical components of the response.

Thus, the mutual coupling effect changes the SSA from a polarization insensitive array to a polarization sensitive one. The polarization sensitivity property of an SSA makes it possible to estimate the polarization parameters of its incident signals.

The mutual coupling effect is a complicated phenomenon, and dependent on the array structure, the type of antennas employed and the angle of arrival of the signals [21][22]. Although it is possible to measure it for some special scenarios, in general, the EM full-wave simulation software is employed to obtain the horizontal and vertical components of the embedded beam pattern of each antenna [23].

The polarization sensitivity of an SSA can be quantified by the parameter *r*, defined as $r = \sigma_1/\sigma_2 \in [0,1]$, where σ_1 and σ_2 are the singular values of the manifold matrix $\boldsymbol{A}(\theta,\varphi)$. As mentioned, the manifold matrix without mutual coupling does not contain any polarization information and $\boldsymbol{A}(\theta,\varphi)$ is a rank-1 matrix for $r = 0$, while for $r \neq 0$, $\boldsymbol{A}(\theta,\varphi)$ becomes a rank-2 matrix with polarization information.

3. PARAMETER ESTIMATION ALGORITHM

First define the covariance matrix of the array output as

$$\begin{aligned}\boldsymbol{R} &= E\left[\boldsymbol{x}(t)\boldsymbol{x}^H(t)\right] \\ &= \sum_{k=1}^{K} \boldsymbol{A}(\theta_k,\varphi_k)\boldsymbol{p}\left(\alpha_k,\beta_k\right)\boldsymbol{R}_s\boldsymbol{p}^{\mathrm{H}}\left(\alpha_k,\beta_k\right)\boldsymbol{A}^{\mathrm{H}}(\theta_k,\varphi_k) + \sigma^2\boldsymbol{I}_{\mathrm{M}}\end{aligned} \tag{8}$$

where $\boldsymbol{R}_s = E[\boldsymbol{s}(t)\boldsymbol{s}^H(t)]$ is the signal covariance matrix, $\boldsymbol{s}(t) = [s_1(t)...s_K(t)]^T$ is the signal vector, $E[\bullet]$ denotes the expectation operation and σ^2 is the noise variance.

In practice, $\boldsymbol{R}$ is estimated by a finite number of snapshots *L* as follows,

$$\hat{\boldsymbol{R}} = \frac{1}{L}\sum_{l=1}^{L}\boldsymbol{x}(l)\boldsymbol{x}^H(l) \tag{9}$$

Suppose the signal number *K* is known or can be estimated in advance, the MUSIC algorithm can be applied to find the signal parameters by searching for peaks of the following cost function

$$S(\theta,\varphi,\alpha,\beta) = \frac{1}{\boldsymbol{a}_P^H(\theta,\varphi,\alpha,\beta)\boldsymbol{U}_n\boldsymbol{U}_n^H\boldsymbol{a}_P(\theta,\varphi,\alpha,\beta)} \tag{10}$$

where $\boldsymbol{U}_n$ is the noise subspace composed of (*M*-*K*) non-dominant vectors of the singular value decomposition (SVD) of $\hat{\boldsymbol{R}}$ [15], and $\boldsymbol{a}_P(\theta,\varphi,\alpha,\beta) = \boldsymbol{A}(\theta,\varphi)\boldsymbol{p}(\alpha,\beta)$.

The 4-D peak search involved in (10) has a very high computational complexity. To reduce the complexity, in the following, we decompose it into two separate 2-D estimation problems in a similar way as in [17].

The manifold matrix $\boldsymbol{a}_P$ is orthogonal to the noise subspace $\boldsymbol{U}_n$, i.e.

$$\boldsymbol{U}_n{}^H\boldsymbol{a}_P = \boldsymbol{0} \tag{11}$$

By separating $\boldsymbol{a}_P(\theta,\varphi,\alpha,\beta)$ into the DOA component and the polarization component, (11) can be expressed as

$$\boldsymbol{U}_n{}^H(\boldsymbol{A}\boldsymbol{p}) = (\boldsymbol{U}_n{}^H\boldsymbol{A})\boldsymbol{p} = \boldsymbol{0} \tag{12}$$

Since $\boldsymbol{U}_n{}^H\boldsymbol{A}$ is an $(M-K)\times 2$ vector and $\boldsymbol{p}$ is a 2×1 vector, (12) shows a linear relationship between the columns in $\boldsymbol{U}_n{}^H\boldsymbol{A}$, which means $\boldsymbol{U}_n{}^H\boldsymbol{A}$ has a column rank less than 2. Then, the determinant of the 2×2 matrix $\boldsymbol{A}^H\boldsymbol{U}_n\boldsymbol{U}_n{}^H\boldsymbol{A}$ is equal to zero, which is given by

$$\mathbf{det}(\boldsymbol{A}^H\boldsymbol{U}_n\boldsymbol{U}_n{}^H\boldsymbol{A}) = 0 \tag{13}$$

where **det(**□**)** denotes the determinant of a matrix.

As a result, the DOA estimator can be established as

$$S(\theta,\varphi) = \frac{1}{\mathbf{det}(\boldsymbol{A}^H\boldsymbol{U}_n\boldsymbol{U}_n{}^H\boldsymbol{A})} \tag{14}$$

After performing a 2-D peak search over the DOA parameters, with the DOA estimation result, the polarization parameters can be obtained by another 2-D search

$$S(\alpha,\beta) = \frac{1}{\boldsymbol{p}^H\boldsymbol{A}^H\boldsymbol{U}_n\boldsymbol{U}_n{}^H\boldsymbol{A}\boldsymbol{p}} \tag{15}$$

4. SIMULATION AND DISCUSSION

In this section, the feasibility of polarization estimation based on an SSA is demonstrated and the relationship between the polarization estimation performance and the array polarization sensitivity is analyzed. A 16-element planar right-handed circularly polarized array with double-patch microstrip element antenna in Ku-band is shown in Fig. 3. The distance between adjacent elements is set as d=0.45λ.

All the horizontal and vertical components of the individual beam pattern are exported by running the electromagnetic simulation software Ansys HFSS [18]. The root mean square error (RMSE) is defined as

$$\mathrm{RMSE} = \left(\frac{1}{KC}\sum_{k=1}^{K}\sum_{c=1}^{C}\mathrm{E}[(\overline{\eta}-\eta)^2]\right)^{1/2} \tag{16}$$

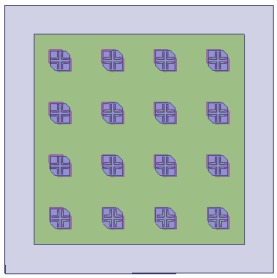

Fig. 3. The planar array with 16 right circularly polarized microstrip antennas.

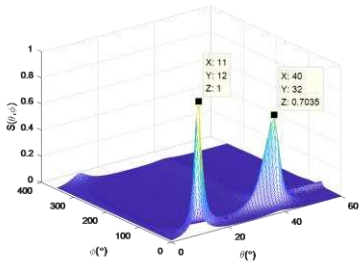

Fig. 4. Normalized DOA spectrum of two impinging signals.

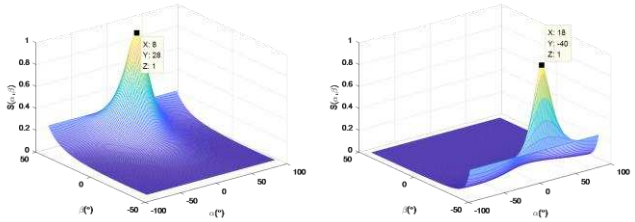

(a). Signal from $(40°, 35°)$ **(b).** Signal from $(10°, 10°)$

Fig. 5. Polarization spectrums of two impinging signals.

where $\overline{\eta} = \{\overline{\alpha}, \overline{\beta}\}$ and $\eta = \{\alpha, \beta\}$ denote the estimated and the actual polarization parameters, respectively, and C represents the number of Monte Carlo experiments, which is 500 in the following simulations. Suppose the boresight signal to noise ratio (SNR) is 5 dB and the number of snapshots for estimating the noise subspace $\boldsymbol{U}_n$ is 1000.

Firstly, two uncorrelated signals from $(\theta, \varphi) = (40°, 35°)$ and $(10°, 10°)$ with polarization parameters $(\alpha, \beta) = (10°, 30°)$ and $(20°, -40°)$ are considered. The DOA spectrum obtained by (14) is shown in Fig. 4 with the peak value $(40°, 32°)$ and $(11°, 12°)$. Then a 2-D search for polarization parameters is employed by (15) under the estimated DOA results, and the result is shown in Fig. 5 (a) and (b). It can be seen that the estimated polarization parameters are $(8°, 28°)$ and $(18°, -40°)$, which are very close to the true values.

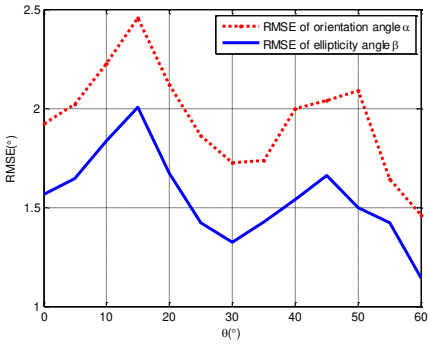

Fig. 6. RMSE for polarization parameters versus θ.

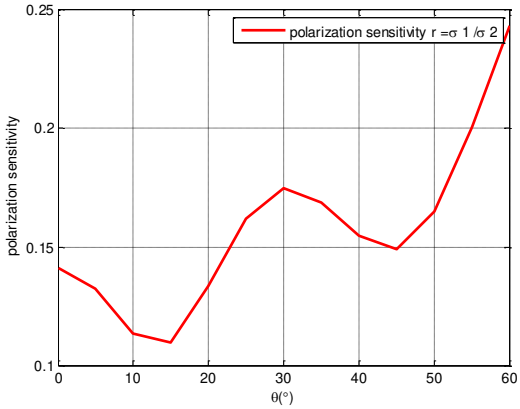

Fig. 7. Polarization sensitivity of SSA at different angles.

Next, the relationship between polarization estimation performance and array polarization sensitivity is studied. Since the manifold matrix with polarization sensitivity is direction dependent, the polarization estimation performance will be analyzed in a range of angle regions. In the following simulation, the azimuth angle of the impinging signal is fixed at $\varphi = 0°$ and the elevation angle varies from $\theta = 0°$ to $\theta = 60°$ with the signal polarization parameter $(\alpha, \beta) = (0°, 20°)$. The RMSE for polarization parameter estimation and the degree of array polarization sensitivity with respect to the change of elevation angle is demonstrated in Figs. 6 and 7, respectively. The peak of the RMSE curve corresponds to the valley of the polarization sensitivity curve and vice versa. Considering the decrease of antenna gain in those large off-boresight angles, the close relationship between polarization estimation accuracy and polarization sensitivity can be established: the higher the polarization sensitivity is, the lower the RMSE of the estimated polarization parameter.

5. CONCLUSION

In this paper, the feasibility of polarization estimation based on the traditional scalar antenna array has been studied and demonstrated by computer simulations. The mutual coupling effect, normally considered as a disadvantage in antenna array design, transforms the SSA into a polarization-sensitive array and therefore can be employed for estimating the polarization information of the impinging signals. A dimension-reduction based MUSIC algorithm is developed to estimate all the four signal parameters effectively. As an example, a planar array of 16 right circularly polarized microstrip antennas was employed and the results show a close relationship between polarization estimation accuracy and the polarization sensitivity of the array. The theoretical performance of the dimension-reduction MUSIC for SSA will be derived in the subsequent research.

6. REFERENCES

[1] A. J. Weiss and B. Friedlander, "Performance analysis of diversely polarized antenna arrays," *IEEE Transactions on Signal Processing* vol. 39, no 7, pp. 1589-1603, 1991.

[2] W. Liu, "Channel equalization and beamforming for quaternion-valued wireless communication systems," *Journal of the Franklin Institute*, vol. 354, issue 18, pp. 8721–8733, December 2017.

[3] N. F. Chamberlain, E. K. Walton, and F. D. Garber, "Radar target identification of aircraft using polarization-diverse features," *IEEE Transactions on Aerospace and Electronic Systems*, vol. 27, pp. 58-67, 1991.

[4] X. Cheng, A. Aubry, D. Ciuonzo, A. De Maio, X. Wang, "Robust waveform and filter bank design of polarimetric radar", *IEEE Trans. Aerosp. Electron. Syst.*, vol. 53, no. 1, pp. 370-384, Feb. 2017.

[5] H. Krim and M. Viberg, "Two decades of array signal processing research: The parametric approach," *IEEE Signal Process. Mag.*, vol. 13, no. 4, pp. 67–94, Jul. 1996.

[6] B. Friedlander, "Antenna array manifolds for high-resolution direction finding," *IEEE Transactions on Signal Processing*, vol. 66, no. 4, pp. 923–932, Feb. 2018.

[7] H. L. Van Trees, *Optimum Array Processing, Part IV of Detection, Estimation, and Modulation Theory*. New York, NY, USA: Wiley, 2002.

[8] J. Li, R. T. Compton, "Angle and polarization estimation using ESPRIT with a polarization sensitive array," *IEEE Trans. Antennas Propag.*, vol. 39, no. 9, pp. 1376-1383, Sep 1991.

[9] A. Nehorai, E. Paldi, "Vector-sensor array processing for electromagnetic source localization," *IEEE Transactions on Signal Processing*, vol. 42, no. 2, pp. 376-398, Feb. 1994.

[10] K.T. Wong and M.D. Zoltowski, "Closed-form direction finding and polarization estimation with arbitrarily spaced electromagnetic vector-sensors at unknown locations," *IEEE Trans. Antennas Propag.*, vol. 48, pp. 671-681, May 2000.

[11] X. Lan and W. Liu, "Fully quaternion-valued adaptive beamforming based on crossed-dipole arrays," Electronics, vol. 6, no. 2, p. 34, 2017.

[12] M. D. Jiang, Y. Li, and W. Liu, "Properties of a general quaternion-valued gradient operator and its application to signal processing," Frontiers of Information Technology & Electronic Engineering, vol. 17, pp. 83–95, February 2016.

[13] B. Friedlander, "Polarization sensitivity of antenna arrays," *IEEE Transactions on Signal Processing*, vol. 67, no. 1, pp. 234-244, 2019.

[14] I J. Gupta and A.A. Ksienski, "Effect of Mutual Coupling on the Performance of Adaptive Arrays," *IEEE Trans. Antennas Propag.*, vol. AP-31, no. 5, pp. 785-791, September 1983.

[15] R. O. Schmidt, "Multiple emitter location and signal parameter estimation," *IEEE Trans. Antennas Propag.*, vol. 34, no. 3, pp. 276-280, 1986.

[16] P. Stoica and A. Nehorai, "MUSIC, maximum likelihood and Cramir-Rao bound,'' *IEEE Trans. Acoust., Speech, Signal Processing*, vol. 37, pp. 720-741, May 1989

[17] X. Lan, W. Liu, and H. Y. T. Ngan, "Joint 4-D DOA and polarization estimation based on linear tripole arrays," Proc. the International Conference on Digital Signal Processing, London, UK, Aug. 2017.

[18] [Online]. Available: https://www.ansys.com/en-gb/products/electronics/ansys-hfss.

[19] C. A. Balanis, *Antenna Theory - Analysis and Design*, 3rd edition, John Wiley & Sons, 2005.

[20] B. Fuchs and J.J. Fuchs, "Optimal polarization synthesis of arbitrary arrays with focused power pattern," *IEEE Trans. Antennas Propag.*, vol. 59, no. 12, pp. 4512-4519, 2011.

[21] H. Steyskal and J. S. Herd, "Mutual coupling compensation in small array antennas," *IEEE Trans. Antennas Propag.*, vol. 38, no. 12, pp. 1971-1975, 1990.

[22] D. M. Pozar, "Input impedance and mutual coupling of rectangular microstrip antennas," *IEEE Trans. Antennas and Propag.*, vol. 30, pp. 1191-1196, Nov. 1982.

[23] J. S. Row and Y. J. Huang, "Reconfigurable antenna with switchable broadside and conical beams and switchable linear polarized patterns," *IEEE Trans. Antennas Propag.*, vol. 66, no. 7, pp. 3752-3756, Jul. 2018.